NIH Public Access
Author Manuscript
Mol Microbiol. Author manuscript; available in PMC 2012 January 1.

Published in final edited form as:
Mol Microbiol. 2011 January ; 79(1): 133–148. doi:10.1111/j.1365-2958.2010.07431.x.

A Novel Copper-Responsive Regulon in *Mycobacterium tuberculosis*

Richard A. Festa[1], **Marcus B. Jones**[2], **Susan Butler-Wu**[1,3], **Daniel Sinsimer**[1,4], **Russell Gerads**[5], **William R. Bishai**[6], **Scott N. Peterson**[2], and **K. Heran Darwin**[1,*]

[1]New York University School of Medicine, Department of Microbiology, 550 First Avenue MSB 236, New York, NY 10016 USA

[2]Pathogen Genomics Resource Center (PFGRC), J. Craig Venter Institute (JCVI), 9704 Medical Center Drive, Rockville, MD 20850 USA

[5]Applied Speciation and Consulting, LLC, 18804 Northcreek Parkway, Bothell, WA 98011 USA

[6]Johns Hopkins School of Medicine, Department of Medicine, Division of Infectious Diseases, 1550 Orleans St. Room 108, Baltimore, MD 21231 USA

Abstract

In this work we describe the identification of a copper-inducible regulon in *Mycobacterium tuberculosis* (*Mtb*). Among the regulated genes was Rv0190/MT0200, a paralogue of the copper metalloregulatory repressor CsoR. The five-locus regulon, which includes a gene that encodes the copper-protective metallothionein MymT, was highly induced in wild type *Mtb* treated with copper, and highly expressed in an Rv0190/MT0200 mutant. Importantly, the Rv0190/MT0200 mutant was hyper-resistant to copper. The promoters of all five loci share a palindromic motif that was recognized by the gene product of Rv0190/MT0200. For this reason we named Rv0190/MT0200 RicR for *r*egulated *i*n *c*opper *r*epressor. Intriguingly, several of the RicR-regulated genes, including MymT, are unique to pathogenic *Mycobacteria*. The identification of a copper-responsive regulon specific to virulent mycobacterial species suggests copper homeostasis must be maintained during an infection. Alternatively, copper may provide a cue for the expression of genes unrelated to metal homeostasis, but nonetheless necessary for survival in a host.

Introduction

Mtb is the causative agent of tuberculosis and infects an estimated nine million people per year. One to two million people die from tuberculosis each year, making *Mtb* one of the most deadly infectious agents in the world (http://www.who.int/tb/publications/global_report/2009/update/en/index.html). Infection occurs upon inhalation of aerosolized droplets containing *Mtb* bacilli. Left untreated, most infections do not immediately lead to disease, but rather remain latent for many years [reviewed in (Saunders & Britton, 2007)]. *Mtb* has evolved to survive inside macrophages where it faces a multitude of stresses, including reactive nitrogen and oxygen intermediates (RNI, ROI), acidification of the phagosome, and iron limitation [reviewed in (Flynn & Chan, 2001, Pieters, 2008)].

[*]To whom correspondence should be addressed: heran.darwin@med.nyu.edu, Tel.: (212) 263-2624, Fax: (212) 263-8276.
[3]Current address: University of Washington Medical Center, Clinical Microbiology Laboratory, 1959 NE Pacific Street, NW120, Seattle, WA 98195-7110 USA
[4]Current address: University of Medicine and Dentistry of New Jersey-Robert Wood Johnson Medical School, Child Health Institute of New Jersey, 89 French Street, 4th Floor, New Brunswick, NJ 08901 USA

NIH-PA Author Manuscript
NIH-PA Author Manuscript
NIH-PA Author Manuscript

NIH-PA Author Manuscript

NIH-PA Author Manuscript

NIH-PA Author Manuscript

While host-inflicted stresses are typically bactericidal, *Mtb* has developed ways to resist elimination by these defense mechanisms. Previous studies revealed that the *Mtb* proteasome is necessary for the bacteria to resist RNI toxicity in vitro and cause lethal infections in mice [reviewed in (Darwin, 2009)]. Proteasomes are barrel-shaped compartmentalized proteases that degrade proteins in a highly regulated manner [reviewed in (Cerda-Maira & Darwin, 2009)]. *Mtb* proteasome function requires Mpa (M*ycobacterium p*roteasomal *A*TPase), a hexameric ATPase that unfolds and translocates substrates into the proteasome core (Darwin *et al.*, 2005, Pearce *et al.*, 2006, Striebel *et al.*, 2010) and PafA (*p*roteasome *a*ccessory *f*actor *A*), which ligates the small post-translational modifier Pup (*p*rokaryotic *u*biquitin-like *p*rotein) to proteins, dooming them for degradation (Festa *et al.*, 2007, Pearce *et al.*, 2008, Striebel *et al.*, 2009). Despite significant progress in characterizing the biochemistry of the *Mtb* proteasome system, it is not known how proteolysis is linked to *Mtb* resistance to RNI or virulence.

In an effort to begin to understand the link between *Mtb* proteasome function and pathogenesis, we sought to determine the role of the proteasome in transcriptional regulation. Compartmentalized proteases are often involved in regulating the stability of transcription factors, either directly or indirectly [reviewed in (Gottesman, 2003, Collins & Tansey, 2006)]. Notably, non-proteasomal, self-compartmentalized proteases have been implicated in virulence gene expression in bacterial pathogens [reviewed in (Butler *et al.*, 2006)]. Based on these observations, we used *pafA* and *mpa* mutants to look for proteasomal degradation-dependent transcriptional changes that might reveal pathways important for pathogenesis. Under normal culture conditions, we observed significant changes in gene expression in less than 2% of the 4,009 predicted open reading frames (orfs) in *pafA* and *mpa* mutants compared to wild type (WT) *Mtb*. From this analysis, we identified a previously unrecognized copper responsive regulon. This regulon is controlled by RicR (GenBank accession number GU726749), a homologue of the *Mtb c*opper-sensitive *o*peron *r*epressor, CsoR (Liu *et al.*, 2007). Disruption of *ricR* resulted in the constitutive expression of the entire regulon and hyper-resistance of *Mtb* to copper. In contrast, CsoR regulated only a single operon that includes *csoR* and a putative copper transporter gene, *ctpV* (cation transporter P-type ATPase). Thus, our studies showed that defects in proteasome-dependent degradation result in transcriptional changes in *Mtb*. Furthermore, there appears to be at least two independent pathways to respond to copper-mediated stress, which may be critical during infection of a host.

Results

Transcriptional profiles of proteasome degradation-defective *Mtb*

We sought to identify genes that were regulated in a proteasome-dependent manner by comparing the transcriptomes of WT *Mtb* with *pafA* or *mpa* mutant strains (Table S1 for strain information). We did not analyze proteasome protease-disrupted *Mtb* because genetic or chemical disruption of protease activity results in a general growth defect (Gandotra *et al.*, 2007,Darwin *et al.*, 2003), which is not observed for *mpa* or *pafA* mutants (Darwin et al., 2003). Because PafA and Mpa are both involved in the Pup-proteasome degradation pathway, we hypothesized that the transcriptional profiles of *pafA* and *mpa* mutants would be similar. We also analyzed the transcriptome of a mutant with a transposon insertion in the penultimate codon of *mpa* ("*mpa607*"), which results in the synthesis of an Mpa allele with ATPase activity but unable to facilitate protein degradation (Darwin et al., 2003,Pearce et al., 2006). Therefore, we analyzed the *mpa607* mutant to determine if it had a different transcriptional profile from an *mpa* transposon null mutant.

RNA for microarray analysis was harvested at mid-log [optical density absorbance at 580 nm (OD_{580}) = 0.4] and early stationary (OD_{580} = 2.0) phases (see *Experimental*

NIH-PA Author Manuscript

NIH-PA Author Manuscript

NIH-PA Author Manuscript

Procedures). Genes were considered significantly regulated if the change in transcript levels was greater than 2-fold after significance analysis of microarrays (SAM) analysis comparing all four transcriptomes (Kooperberg *et al.*, 2002). Data from the mid-log cultures showed either minimal change (less than 2-fold) in the transcriptional profiles between strains, or were high variability among experiments (data not shown). The microarray results from early stationary phase were more consistent and therefore used for further studies and validation. We observed similar transcriptional profiles between all three mutants (*pafA*, *mpa*, *mpa607*) suggesting that PafA and Mpa do not have independent roles that lead to differing transcriptional responses under the conditions tested (Tables 1, 2, and S2; Geo Accession GSE23947).

Many genes in the Zur (zinc uptake regulator, Rv2359) regulon were up-regulated in the *pafA* and *mpa* mutants (Maciag *et al.*, 2007) (Table 1). When zinc is low, Zur is released from its operators and gene expression is induced. The induced genes presumably aid the bacteria during zinc-limiting conditions. Among the Zur-regulated genes was the *esx-3* (esat-6, region 3) operon, which is also controlled by IdeR (iron dependant repressor, Rv2711) (Rodriguez *et al.*, 2002), and is important for iron uptake during iron-limiting conditions (Serafini *et al.*, 2009, Siegrist *et al.*, 2009). IdeR directly represses the *esx-3* locus, but does not appear to regulate other Zur regulon genes (Maciag et al., 2007, Rodriguez et al., 2002). IdeR-dependent/Zur-independent genes (Gold *et al.*, 2001) were not differentially expressed between the WT and *mpa* or *pafA* mutants, suggesting that the changes in *esx-3* transcript levels were due to effects through Zur rather than IdeR. Notably, *zur* transcript levels were unchanged in all strains tested (Table 1, Geo Accession GSE23947).

We hypothesized that decreased intracellular levels of zinc in the *pafA* and *mpa* mutants resulted in the de-repression of the Zur regulon. To attempt to address this, we performed inductively coupled plasma dynamic reaction cell mass spectrometry (ICP-DRC-MS) to quantify intracellular zinc amounts. It is important to note that vanishingly small amounts of buffered or bio-available zinc are present within a cell; zinc-coordinating enzymes and ribosomes largely sequester zinc (Hitomi *et al.*, 2001). The ICP-DRC-MS results indicated that total zinc concentrations in the WT and degradation-defective *Mtb* strains were relatively similar between samples and biological replicates (Fig. S1). It is notable that *E. coli* Zur can respond to less than femtomolar changes in free zinc, much like other zinc metalloregulatory proteins (Outten & O'Halloran, 2001, Ma *et al.*, 2009c), and our analysis might not have been sensitive enough to detect small but significant alterations in the concentration of bio-available or rapidly exchanging zinc. Thus, it remains to be determined how disruption of proteasome function affects Zur-dependent transcription.

Identification of a regulatory element controlling promoters repressed in proteasome degradation-defective *Mtb*

Unlike the up-regulated genes, the down-regulated genes did not share a known regulatory mechanism. Most of these genes were unlinked and encoded hypothetical proteins (Table 2). Because the same transcriptional regulator typically controls co-regulated genes, we examined the putative promoter regions of all down-regulated genes in an attempt to identify a common regulator binding site. A palindrome, 5'-TACCC-N_5-G/AGGTA-3', was identified upstream of *lpqS* (putative lipoprotein; Rv0847) and Rv2963 (putative permease) (Fig. 1A). To determine if these palindromes were located near transcriptional start sites, we performed rapid amplification of 5' complementary DNA ends (5'RACE) for both genes. The palindrome was between or overlapped tentative −10/−35 regions of each promoter, which strongly suggested the mechanism of transcriptional control was through the action of a repressor.

NIH-PA Author Manuscript

NIH-PA Author Manuscript

NIH-PA Author Manuscript

To determine if other promoters contained this regulatory element, we searched for this palindrome in the *Mtb* genome using the Search Pattern tool on GenoList (http://genodb.pasteur.fr). We performed a stringent search using the sequence 5'-TACCCNNNNNGGGTA-3' and allowed for two mismatches. Three additional loci with this palindrome were identified: one upstream of a gene annotated as a "conserved hypothetical" (Rv0190, herein called *ricR*) and previously identified as a copper responsive gene (Ward *et al.*, 2008); one upstream of *mymT* (encoding a copper metallothionein) (Gold *et al.*, 2008); and the other in a region between *ppe23* (Rv1706c) and Rv1706A (Fig. 1A). Upon closer examination, the palindrome near *ppe23* was actually upstream of two small orfs: "*orfA*" and "*orfB*" were 186 bp and 165 bp, respectively, in length. Neither was annotated in H37Rv but *orfB* was annotated in the CDC1551 genome sequence as MT1746.1. A transcript corresponding to the *orfAB* operon was detected in *Mtb* H37Rv (Fig. S2).

5'RACE analysis suggested that the palindrome was between tentative −10/−35 sites of *ricR*, *mymT* and *orfAB* as observed for *lpqS* and Rv2963 (Fig. 1A). Upon further inspection of the microarray data, we found *mymT* was indeed down-regulated in the *mpa* and *pafA* mutants, but less than two-fold (Table 2). *ricR* and MT1746.1 were not identified in the microarray data (Geo Accession GSE23947), but it was possible that the changes in transcript levels were not consistent among experiments based on the statistical analysis of microarrays (SAM) analysis. Nonetheless, quantitative real time PCR (qRTPCR) analysis showed transcript levels of *ricR*, *mymT*, and *orfAB* were decreased in the *pafA* and *mpa* mutants as observed for *lpqS* and Rv2963 (Fig. 1B). Complementation of the *mpa* mutation resulted in the restoration of near WT expression of these genes (Fig. 1C).

lpqS, *mymT* and *orfAB* are only found in pathogenic mycobacteria, suggesting they play a role in host-pathogen interactions (Fig. 1D). LpqS homologues with greater than 50% identity are only found in three other sequenced species, *M. kansasii*, *M. marinum* and *M. ulcerans*. *orfAB* is present only in the *Mtb* complex, which includes *M. bovis*. Among *Mycobacteria*, Rv2963 is only found among pathogenic species although homologues with lower similarity are present in other bacterial genera. In contrast, RicR homologues are present in many bacterial species. Taken together, we identified five loci that share a palindrome in their promoters, suggesting they are controlled by a common regulatory mechanism.

Identification of a copper-inducible regulon

A previous report by Ward and co-workers identified numerous genes that are differentially regulated in *Mtb* treated with copper (Ward *et al.*, 2008). Among these genes, Rv2963 and *ricR* were induced 15.7- and 8.5-fold, respectively (Ward et al., 2008). A gene downstream of *lpqS*, Rv0848, was also induced by copper (Ward et al., 2008). Metallothioneins are synthesized upon metal stress to bind excess zinc or copper (Sato & Bremner, 1993); consistent with this *mymT* is also highly induced by copper and other metals (Gold et al., 2008). Based on these observations, we decided to test if *lpqS* and *orfAB*, along with *mymT*, Rv2963 and *ricR*, were also copper inducible. After growing WT *Mtb* in Sauton's minimal media to stationary phase (OD_{580} = 1.5) and treating with 500 μM copper sulfate ($CuSO_4$) for four hours, we found that all five loci were induced by copper (Figure 2A). Because *orfAB* was not previously annotated, we now refer to this operon as *socAB* (small *o*rf induced by *c*opper A and B; GenBank accession number HM222605). As an additional control for copper induction, we measured the expression of two previously characterized copper-inducible genes, *csoR* and *ctpV* (Liu et al., 2007, Ward et al., 2008). As expected, copper induction was observed for both of these genes (Fig. 2A).

NIH-PA Author Manuscript

NIH-PA Author Manuscript

NIH-PA Author Manuscript

To test the metal specificity of this regulon, we treated WT *Mtb* with other biologically relevant metals (manganese, iron, cobalt, nickel, and zinc) or silver and measured the expression of all five genes. None of the genes was induced by manganese, cobalt, nickel and silver (data not shown). In contrast, all genes were induced to varying degrees by iron or zinc (Fig. 2B). Consistent with our data, *mymT* is induced by metals in addition to copper (Gold et al., 2008). While this increase was significant over untreated samples, it is unclear if iron or zinc specifically induced these promoters.

We hypothesized that *lpqS*, Rv2963, *mymT*, *socAB*, and *ricR* were down-regulated in the *pafA* and *mpa* mutants when compared to WT because these strains had lower intracellular copper concentrations. As with zinc, ICP-DRC-MS experiments showed that copper was not significantly reduced in any of the strains (Fig. S1). Thus, it remains unclear how defects in proteasome function affect the expression of these copper-inducible genes.

RicR is a copper responsive regulator

We hypothesized that the palindrome identified in the promoters of *lpqS*, Rv2963, *mymT*, *ricR*, and *socAB* was a repressor-binding site. Thus our next aim was to identify the repressor that controlled this regulon. We first tested CsoR as the possible repressor. The *cso* operon, consisting of *csoR*, Rv0968, *ctpV* and Rv0970, is de-repressed in the presence of copper as CsoR dissociates from its operator upon copper binding (Liu et al., 2007). However, it was not known if CsoR regulated other loci in *Mtb*. To determine whether or not CsoR was the regulator of the newly recognized regulon, we used microarrays to compare the transcriptomes of WT and *csoR*-deleted/disrupted (Δ*csoR::hyg*) *Mtb* (see *Experimental Procedures*). Because we were measuring the expression of genes physically unlinked to *csoR*, we were not concerned about polar effects caused by the hygromycin gene disrupting *csoR*.

In Sauton's minimal media without added copper, the expression of genes downstream of *csoR* (Rv0968, *ctpV*, Rv0970) in the Δ*csoR::hyg* mutant were slightly elevated compared to WT *Mtb* grown to stationary phase (OD_{580} ~1.5) (Tables 3 and S3, Geo Accession GSE23498). If we had introduced an in frame, unmarked deletion mutation in *csoR*, we would have expected to see a high level of expression of the *cso* operon due to the absence of its cognate repressor. However, because of the likely polar nature of the mutation we introduced into *csoR*, we did not observe this. We thus predicted that the addition of $CuSO_4$ would not increase the expression of the *cso* operon in the Δ*csoR::hyg* mutant. Upon supplementation of the growth media with 500 μM $CuSO_4$ and incubation for four hours, the *cso* operon was strongly induced in WT *Mtb* but not in the Δ*csoR::hyg* mutant, consistent with our prediction (Table 3). Interestingly, no other genes appeared to be differentially regulated between the WT and Δ*csoR::hyg* strains, suggesting CsoR only regulates its own promoter under the conditions tested. Importantly, *lpqS*, Rv2963, *mymT*, *ricR*, and *socAB* expression was not altered in the Δ*csoR::hyg* mutant, which was confirmed by qRTPCR (Fig. S3B). Thus, CsoR was not the regulator of the five copper-regulated loci that were repressed in the proteasome degradation-defective *Mtb* strains.

It was previously noted that RicR and CsoR are predicted to share the same overall structure and amino acids required for reduced copper [Cu(I)] coordination and allosteric regulation of DNA binding (Liu et al., 2007, Ma *et al.*, 2009b) (Fig. 3A). The major difference between the two proteins is that *Mtb* CsoR has an extended C-terminal tail that is required for high affinity *cso* operator binding (Ma et al., 2009b). In fact, RicR is more similar to the only other well-characterized CsoR homologue, *Bacillus subtilis* CsoR (51% with *Bsu*CsoR), which does not have the extended C-terminus found in *Mtb* CsoR (Smaldone & Helmann, 2007, Ma *et al.*, 2009a). Furthermore, the *Bsu*CsoR binding site is nearly identical to the palindrome identified upstream of *lpqS*.

NIH-PA Author Manuscript

NIH-PA Author Manuscript

NIH-PA Author Manuscript

To determine if RicR regulated the five gene copper-responsive regulon, we examined the expression profile of a previously uncharacterized ΦMycoMarT7 transposon mutant of *ricR* in *Mtb* strain CDC1551. We determined that the mutant had a growth defect under standard culture conditions (7H9 broth, Fig. 3B, top) as well as in Sauton's minimal media without added copper (Fig. 3B, bottom); we thus harvested bacteria for qRTPCR analysis at an OD_{580} of ~0.6. If RicR were a repressor controlling its own expression as well as the transcription of *lpqS*, Rv2963, *mymT*, and *socAB*, a *ricR* mutation should result in copper-independent constitutive expression of these genes. Indeed, all genes were highly expressed in the *ricR* mutant compared to WT *Mtb* grown in Sauton's minimal media without added copper (Fig. 3C). Additionally, the expression of these genes in the *ricR* mutant was comparable to the expression observed in WT *Mtb* treated with 500 μM $CuSO_4$ for four hours (Fig. 3C).

Finally, we complemented the *ricR* transposon mutation in single copy with *ricR* expressed from its native promoter. While RicR levels were partially restored (Fig. 4A), *lpqS* expression was repressed to WT levels (Fig. 4B). In addition, MymT levels, which drastically increased in the *ricR* mutant, were also restored to undetectable WT amounts in the complemented strain (Fig. 4C).

To determine if RicR regulated other genes, we performed microarray analysis comparing the *ricR* transposon mutant to WT *Mtb* (Geo Accession GSE23498, Table S4). We grew cultures to an OD_{580} of ~0.6 in Sauton's minimal media containing no added copper. As expected, the most highly expressed genes in the *ricR* mutant were *lpqS*, Rv2963, *mymT*, and *socAB* (Table 4). *ricR* was also highly expressed, supporting the hypothesis that *ricR* is autoregulated. Transcription of *ricR* could be observed by microarray analysis because the oligonucleotide designed for the microarrays corresponded to sequence upstream of the transposon insertion, whereas the qRTPCR primers were designed to span the insertion site. Importantly, the difference in expression of all genes diminished between the WT and *ricR* strains upon treatment with 500 μM $CuSO_4$ for four hours (Table 4). Taken together, these data supported the hypothesis that RicR is the copper-inducible repressor of this newly identified regulon.

RicR associates with the *lpqS* promoter palindrome

The next goal was to determine if RicR could associate with DNA encoding the palindrome identified in the *lpqS*, Rv2963, *mymT*, *ricR* and *socAB* promoters. Purified RicR-His_6 could not be maintained in a soluble state upon dilution, and its use in gel-shift assays resulted in non-specific DNA binding (data not shown). As an alternative to using purified protein, we used lysates of *E. coli* producing untagged *Mtb* RicR. Furthermore, rather than using gel retardation, we examined the ability of biotinylated DNA encoding the *lpqS* promoter (*lpqSp*) to co-purify with RicR. RicR robustly co-purified with the *lpqSp* (Fig. 5A). Mutagenesis of a GGGTA interface (5'-TACCC-N5-GTTTA-3') or scrambling of the palindrome sequence disrupted RicR association (Fig. 5A). RicR association appeared to be specific because it did not bind the *csoR* promoter (*csoRp*) or a randomly selected coding DNA sequence (*pks12*) (Fig. 5A). Finally, when copper was added to the reaction we observed a dose-dependent loss of DNA association, which did not occur in the presence of zinc (Fig. 5B). Although we cannot rule out the possibility that an *E. coli* protein bridged RicR to the *lpqSp*, it appears that RicR specifically bound to a palindrome found in the promoters of five loci, and dissociated from DNA in the presence of copper.

The *ricR* mutant is resistant to copper-mediated toxicity

Because the RicR regulon was induced upon exposure to copper, we hypothesized that gene products of this regulon may be needed to combat toxicity related to excess copper levels. In

NIH-PA Author Manuscript

NIH-PA Author Manuscript

NIH-PA Author Manuscript

support of this hypothesis, MymT is required for resistance to copper-mediated toxicity (Gold et al., 2008). Thus, a *ricR* mutant could be more resistant to copper toxicity when compared to WT *Mtb* due to the constitutive expression of *mymT* and the other RicR-regulated genes. We performed a copper sensitivity assay by treating WT, *ricR*, and *ricR*-complemented strains with $CuSO_4$ in microtiter plates (see *Experimental Procedures*). After 10 days, WT and complemented strains grew well in the absence of copper, while the *ricR* mutant grew to a lower density (Fig. 6), consistent with the growth curve analysis (Fig. 3B). The phenotype of strains grown with copper were strikingly reversed: the WT and *ricR*-complemented bacteria were killed by copper in a dose-dependent manner whereas the *ricR* mutant was virtually unaffected by the presence of copper as determined by culture optical density or colony forming units (Fig. 6, Fig. S4,). These data strongly suggested that the constitutive expression of one or more genes in the RicR regulon protected the *ricR* mutant against copper toxicity.

Discussion

In this work, we identified a regulon controlled by the copper-sensing repressor RicR. We propose that under low copper conditions RicR represses gene expression, whereas exposure to excess copper results in RicR dissociation from DNA and the induction of *lpqS*, Rv2963, *mymT*, *socAB* and *ricR*. Consistent with this hypothesis, disruption of *ricR* resulted in the constitutive expression of all five loci in the absence of excess copper. Based on our copper sensitivity assays, we propose that the RicR regulon plays a protective role against copper toxicity. It is also possible that one or more of the regulated genes is not involved in counteracting the effects of copper toxicity, but uses copper as an in vivo cue to trigger gene expression. It is intriguing that RicR regulates several genes that are only found in pathogenic *Mycobacteria*, suggesting that these genes may be required for growth or survival in a specific niche in an animal host.

Of the genes that are controlled by RicR, *mymT* is the only one that has been previously characterized (Gold et al., 2008). MymT is a copper metallothionein that binds up to six Cu(I) ions. As would be predicted for a metallothionein gene, *mymT* is highly induced in the presence of copper (Fig. 2A, 3C) and appears to protect *Mtb* from the toxic effects of copper. However, a *mymT* null mutant is no less virulent than WT *Mtb* in a mouse model of infection (Gold et al., 2008). It is possible that all RicR-regulated genes need to be deleted or constitutively repressed in order to observe a measurable virulence phenotype, a hypothesis we are currently testing. Alternatively, a mouse model of infection may not be appropriate for examining the effects of copper on *Mtb* survival in vivo.

Because the RicR regulon is induced in copper, we propose that gene products in addition to MymT may also play a role in combating copper toxicity. Rv2963 is a putative permease that contains a carboxy(C)-terminus rich in histidines, which can potentially bind copper. LpqS is a probable lipoprotein that also has a histidine-rich region beginning 30 amino acids from its amino(N)-terminus. These histidines are predicted to remain after possible lipoprotein processing and lipidation (Sander *et al.*, 2004). As a putative lipoprotein, LpqS may work with Rv2963 to export copper. That lipoproteins associate with permeases to export ligands has precedence in *Mtb*. LprG (Rv1411c) and Rv1410c transport ethidium bromide (Farrow & Rubin, 2008), while LppX (Rv2945c) is proposed to work with MmpL7 (Rv2942) to export phthiocerol dimycocerosate across the cell membrane (Camacho *et al.*, 1999, Cox *et al.*, 1999).

Divergently expressed from the *lpqS* promoter is Rv0846c, a predicted multi-copper oxidase whose expression is induced by copper (Ward et al., 2008). We also found that it is over-expressed in the *ricR* mutant (Table 4). It is possible that RicR bound to the *lpqSp*

NIH-PA Author Manuscript

NIH-PA Author Manuscript

NIH-PA Author Manuscript

palindrome represses the divergently expressed Rv0846c, especially if RicR, like other metalloregulators, induces long-range changes in DNA structure (Iwig & Chivers, 2009). It was proposed that Rv0846c is chaperoned to the twin-arginine transport system to export copper (Ward et al., 2008); Rv0846c may function like *E. coli* CueO, a "cuproxidase" that oxidizes Cu(I) to the less toxic Cu(II) outside of the cell (Kosman, 2010).

In addition to LpqS and Rv2963, no function has been assigned to the previously unidentified *socAB* operon. Although *socAB* is transcribed (Fig. S2), it is unknown if the message is translated or if it is actually a small non-coding RNA. The role of *socAB* and the other RicR-regulated genes in protecting *Mtb* against copper toxicity is currently under investigation.

Despite the successful identification of the regulator of a new copper responsive regulon, we still do not understand why the RicR regulon is repressed in proteasome degradation-defective *Mtb*. The simplest model is that RicR is itself a proteasome substrate. The accumulation of RicR in the *pafA* and *mpa* mutants might result in the repression of the regulon under normal culture conditions. However, neither endogenous nor ectopically produced RicR levels were altered in proteasome degradation-defective strains under all conditions tested so far (data not shown). Another possibility is that the down-regulation of the RicR regulon in the *mpa* and *pafA* mutants is due to the accumulation of one or more copper-binding proteins that are normally proteasome substrates. This may result in the sequestration of available copper in the cell, mimicking copper-depleted conditions that result in RicR regulon repression. A similar explanation may account for the induction of the Zur regulon, where sequestered zinc would lead to higher gene expression. Ongoing studies are attempting to determine how proteasome activity affects these two metal-dependent regulons.

Prior to our work, CsoR was the only known copper responsive regulator in *Mtb*, controlling the expression of *ctpV*, which encodes a predicted membrane P-type ATPase. CtpV is proposed to be a copper efflux pump based on its regulation by CsoR and its similarity to other copper transporters (Liu et al., 2007). Supporting this hypothesis, a *ctpV* mutant is more susceptible to killing by high levels of copper than WT *Mtb*, presumably because the mutant cannot effectively export copper (Ward *et al.*). Importantly, the *ctpV* mutant is attenuated in an animal infection model, supporting the notion that the maintenance of copper homeostasis is important in vivo. Here, we present data that suggest the RicR regulon, which does not include *ctpV*, is also protective against high levels of copper in vitro. Taken together, we propose that *Mtb* has at least two mutually exclusive but parallel copper inducible pathways controlled by RicR and CsoR (Fig. 7). It remains to be determined if these two pathways represent a redundant response to copper, or if *Mtb* has evolved a graded response to copper toxicity; if so, this would predict that the Cu(I) binding affinities are different for RicR v. CsoR, a hypothesis currently under investigation (B. Keste, D. Giedroc, personal communication).

Little is understood about copper homeostasis during a bacterial infection. The exposure of microbes to excess copper could perhaps act as an innate immune defense, a hypothesis supported by a report suggesting that the mammalian ATP7A, a copper-transporting ATPase, provides some bactericidal activity in macrophages (White *et al.*, 2009). Furthermore, copper levels are elevated in cultured macrophages infected with *Mtb* (Wagner *et al.*, 2005). Copper has long been used as an anti-bacterial agent in laboratory and medical settings (Mikolay *et al.*, 2010), thus perhaps it would not be surprising if animals have developed ways to mobilize cellular copper to battle invading microbes.

NIH-PA Author Manuscript

NIH-PA Author Manuscript

NIH-PA Author Manuscript

Experimental Procedures

Bacterial strains, growth conditions and primers

Bacterial strains, plasmids and primers used in this work are listed in Table S1. Mtb strains were grown in 7H9 broth (Difco) supplemented with 0.2% glycerol, 0.05% Tween-80, 0.5% bovine serum albumin, 0.2% dextrose and 0.085% sodium chloride (ADN), or Sauton's minimal media (3.7 mM potassium phosphate, monobasic; 2.5 mM magnesium sulfate; 30 mM L-asparagine; 3.5 mM zinc sulfate; 9.5 mM citric acid; 6.0% glycerol; 0.005% ferric ammonium citrate; 0.05% Tween 80). Cultures were grown without agitation in 25, 75 or 125 cm^2 vented flasks (Corning) in humidified incubators with 5% CO_2 at 37°C. For growth on solid media, 7H11 agar (Difco) was supplemented with oleic acid, albumin, dextrose and catalase (OADC, BBL). When necessary, H37Rv strains were grown in 50 μg ml^{-1} kanamycin and/or 50 μg ml^{-1} hygromycin. CDC1551 strains were grown in 25μg ml^{-1} kanamycin and/or 25 μg ml^{-1} hygromycin. *E. coli* cultures were grown in Luria Bertani (LB) broth (Difco) on either a rolling drum or shaking at 37°C. LB agar was used for growth on solid medium. Selection was maintained with 200 μg ml^{-1} ampicillin, 100 μg ml^{-1} kanamycin, and 150 μg ml^{-1} hygromycin. Growth curves were performed exactly as described elsewhere (Darwin et al., 2003).

Primers were purchased from Invitrogen. All plasmids were sequenced by GENEWIZ, Inc.

Purification of CsoR and RicR for production of polyclonal antibodies

Purification of CsoR for antibody production was performed under denaturing conditions according to the manufacturer's specifications (Qiagen). RicR was purified under native conditions, and dialyzed in 2 l of phosphate buffered-saline (PBS) at 4°C. Some protein was visibly insoluble after dialysis. Insoluble protein was recovered by centrifugation and washed twice MilliQ water. Protein preparations were about 80% pure and used as the immunogen for RicR antibody production. Polyclonal rabbit antibodies were produced by Covance (Denver, PA). DlaT and MymT antibodies were described previously (Tian *et al.*, 2005, Gold et al., 2008). For immunoblotting analysis, equivalent cell numbers were harvested at the same phase of growth, i.e. when OD_{580} were the same. Bacteria were washed once in an equal volume of PBS with 0.05% Tween 20 and resuspended in 250 μl of lysis buffer (100 mM Tris-Cl, 100 mM potassium chloride, 1 mM EDTA, 5 mM magnesium chloride, pH 8.0). Cells were lysed by bead beating with zirconia beads three times for 30 s. Total cell lysate (150 μl) was mixed with 50 μl of 4× sodium dodecyl sulfate sample buffer and boiled for 10 min. Immunoblotting was performed as previously described (Harlow, 1988). Antibodies to RicR and CsoR were used at a dilution of 1:1,000. Horseradish peroxidase-conjugated goat anti-rabbit antibodies (Pierce) were used for chemiluminescent detection (ThermoScientific SuperSignal West Pico or Femto Chemiluminescent substrate).

Construction of the Δ*csoR*::*hyg* mutant

We made an allelic exchange plasmid to delete and disrupt *csoR* using a plasmid originally developed for specialized transduction (Bardarov *et al.*, 2002). Briefly, approximately 700 bp of DNA upstream and downstream of *csoR* were amplified by PCR and cloned into pYUB854, flanking a hygromycin resistance cassette (see Table S1 for plasmids and primers). The plasmid was linearized with PacI and gel purified. 1 μg of linearized DNA was electroporated into *Mtb* (Hatfull, 2000). Transformants were inoculated onto 7H11+OADC and 50 μg ml^{-1} hygromycin. A no-DNA electroporation control was also inoculated onto the same media to check for spontaneous hygromycin resistance mutants. After three weeks, single colonies were inoculated into 200 μl of 7H9 + ADN in a 96-well plate for one week. The 200 μl starter cultures were used to inoculate a 5 ml cultures for further analysis. The deletion and replacement of *csoR* was confirmed by PCR and

NIH-PA Author Manuscript

NIH-PA Author Manuscript

NIH-PA Author Manuscript

sequencing. Immunoblotting with antibodies raised to *Mtb* CsoR also demonstrated the absence of CsoR (data not shown).

RNA extraction

RNA was extracted from *Mtb* as follows: an equal volume of 4 M guanidinium isothiocyanate (GTC), 0.5% sodium *N*-lauryl sarcosine, 25 mM trisodium citrate) was added to cultures to arrest transcription, and cells were collected by centrifugation at 2,885 *g*. Bacterial were resuspended in 1 ml TRIzol reagent (Invitrogen) and lysed with zirconia silica beads (BioSpec Products) in a BioSpec Mini Bead Beater two times for 30 s, with 1 min cooling on ice in between. Samples were either stored at −80°C or used immediately. Samples were centrifuged for 5 min at 16,100 *g* at 4°C to pellet cellular debris. 300 µl of chloroform was added to PhaseLock tubes (Heavy 2 ml, 5Prime) after which the TRIzol samples were added. Tubes were vigorously inverted for 15 s and allowed to rest at RT for 5 min. Tubes were centrifuged for 10 min at 10,500 *g* at 4°C. The aqueous phases were added to microfuge tubes containing 270 µl isopropanol and 270 µl high salt solution (0.8 M trisodium citrate, 1.2 M NaCl) and vortexed for 5 s. After a 10 min incubation at RT, tubes were microcentrifuged at 16,100 *g* for 10 min at 4°C to pellet RNA. RNA pellets were washed with 1 ml of 75% ethanol and centrifuged at 7,500 *g* for 5 min at 4°C. Pellets were allowed to dry by air and resuspended in 50 µl of RNA storage buffer (Ambion). 2 µl were used for quantification and another 2 µl were added to 80% formamide/ 20% loading dye to check RNA integrity on an (1.6%) agarose gel. The purification process was repeated two times to obtain DNA-free RNA. RNA aliquots were stored at −80°C.

cDNA synthesis, qRTPCR, and 5'RACE

The Reverse Transcription System (Promega) was used to synthesize cDNA from purified RNA. 4 ng of random hexamers (Amersham or Invitrogen) were used to prime cDNA synthesis from 100 ng of RNA as a template. The cDNA equivalent of 1.9 ng of RNA was analyzed by qRTPCR using Platinum SYBR GREEN qPCR SuperMIx UDG (Invitrogen) in a MyIQ2 two-color real-time PCR detection system (Bio-Rad). Analysis was performed using the MyIQ2 software. Normalization for each primer pair was carried out using a standard curve with genomic DNA of known copy number. $\Delta\Delta C_T$ analysis was performed using *rpoB* as a reference gene as previously described (Pearce et al., 2006).

5'RACE was performed as described by the manufacturer (Invitrogen). Briefly, 1 µg of RNA was used as template for cDNA production using a reverse primer 150–300 bp downstream of annotated translational start sites. A 3' poly-C tail was added to cDNA by recombinant Tdt. The cDNA was then amplified using a nested reverse primer and a primer that anneals to the poly-C tail. Products were cloned and sequenced. Likely transcriptional start sites were selected based on clones that had the most sequence upstream of the start codon.

Microarray analysis

The microarray experiments comparing WT, *pafA* and *mpa* strains were grown in 7H9 media supplemented with ADN and RNA was harvested at early stationary phase. Microarrays comparing the *ricR* and *csoR* mutants with WT *Mtb* were performed using RNA harvested from cells grown in Sauton's minimal media to OD_{580} ~0.6 or 1.5, respectively. 500 µM $CuSO_4$ was added to the cultures for four hours for testing copper induction.

Labeled cDNA for microarray experiments were generated by adding 2 µg of total RNA in a mixture containing 6 µg of random hexamers (Invitrogen), 0.01 M dithiothreitol, an aminoallyl-deoxynucleoside triphosphate mixture containing 25 mM each dATP, dCTP, and

NIH-PA Author Manuscript

NIH-PA Author Manuscript

NIH-PA Author Manuscript

dGTP, 15 mM dTTP, and 10 mM amino-allyl-dUTP (aa-dUTP) (Sigma), reaction buffer, and 400 units of SuperScript III reverse transcriptase (Invitrogen) at 42°C overnight. The RNA template was then hydrolyzed by adding sodium hydroxide and EDTA to a final concentration of 0.2 and 0.1 M, respectively, and incubated at 70°C for 15 min. Unincorporated aa-dUTP was removed with a Minelute column (Qiagen). The labeled cDNA was eluted with a phosphate elution buffer (4 mM potassium phosphate, pH 8.5, in ultrapure water), dried, and resuspended in 0.1 M sodium carbonate buffer (pH 9.0). To couple the amino-allyl cDNA with fluorescent labels, normal human serum-Cy3 or normal human serum-Cy5 (Amersham) was added at room temperature for 1 h. Uncoupled label was removed using the Qiagen Minelute column (Valencia, CA). A “dye-flipped” experiment was performed by reversing the coupling of cDNA of Cy3 and Cy5 per experimental pair to control for dye bias. All microarray hybridizations were performed with a minimum of two independent cultures per strain, resulting in at least two dye-flipped experiments per strain pairing.

Aminosilane-coated slides printed with a set of 4750 Mtb oligonucleotides representing all open reading frame sequences (www.jcvi.org) were pre-hybridized in 55 SSC (15 SSC: 0.15 M sodium chloride, 0.015 M sodium citrate; Invitrogen), 0.1% sodium dodecyl sulfate, and 1.0% bovine serum albumin at 42°C for 60 min. The slides were then washed at RT with distilled water, dipped in isopropanol, and allowed to dry. Equal volumes of the appropriate Cy3- and Cy5-labeled cDNA were combined, dried and then resuspended in a solution of 40% formamide, 5×SSC, and 0.1% dodecyl sulfate. Resuspended labeled cDNA were heated to 95°C prior to hybridization. The probe mixture was then added to the microarray slide and allowed to hybridize overnight at 42°C. Hybridized slides were washed sequentially in solutions of 15 SSC-0.2% SDS, 0.15 SSS-0.2% SDS, and 0.15 SSC at RT, then dried in air. All wash buffers were supplemented with 1 ml of 0.1 M DTT per liter of wash buffer. Slides were scanned with an Axon GenePix 4000 scanner and individual TIFF images from each channel were analyzed with TIGR Spotfinder (available at http://pfgrc.jcvi.org/index.php/bioinformatics.html). Microarray data were normalized by LOWESS normalization and with in-slide replicate analysis using the TM4 software MIDAS (available at http://pfgrc.jcvi.org/index.php/bioinformatics.html). We selected genes in which comparison of WT cells exposed to mutants being analyzed yielded $\log_2$ value $|\geq 2.0|$ in all samples. Microarray data can be found at the NCBI Gene Expression Omnibus website (http://www.ncbi.nlm.nih.gov/geo/).

DNA affinity chromatography

DNA probes were made by amplifying sequences of interest with forward primers containing 5’ Biotin TEG modifications (Operon). 50 µl of Dynabeads M-280 Streptavidin (Invitrogen) were washed with 500 µl of 25 B&W buffer (2 M sodium chloride, 1 mM EDTA disodium salt, 10 mM tris hydroxymethyl, pH 7.5) and coupled to 1 µg of biotinylated probe in 15 B&W buffer (200 µl total volume). The bead-DNA mixture was incubated on a rotator at room temperature for 30 min. The coupled beads were then washed once with 500 µl of 15 B&W buffer followed by two washes with buffer A (20 mM Tris-Cl, pH 8.0; 100 mM sodium chloride; 1 mM EDTA disodium salt; 1 mM dithiothreitol (DTT); 10% glycerol). *E. coli* with the pET24b+RicR-Stop plasmid (no His_6 tag) was grown to an optical density (A_{600}) of 0.5 and allowed to grow for three additional hours without induction; leaky expression of *ricR* produced sufficient RicR for experiments. 50 ml of culture was aliquoted and cells were harvested and stored at −20°C until needed. 20 ml were used to prep 10 ml of lysate. Pellets were resuspended in 10 ml of buffer A and snap frozen in an ethanol dry ice bath. After thawing on ice, the cell suspension was sonicated twice for 30 sec (1 second on, 1 second off) with 10 min of icing in between. Lysates were clarified by centrifugation at 10,000 *g* for 30 min. DNA coupled Dynabeads were then added to 1 ml

NIH-PA Author Manuscript

NIH-PA Author Manuscript

NIH-PA Author Manuscript

of clarified lysate and rotated for 30 min at room temperature. After incubation, tubes were centrifuged briefly to collect solution on the bottom of the tubes. The beads were washed in 1 ml buffer A, transferred to a new tube, and subsequently washed 3 more times with 1 ml buffer A. Protein interacting with the coupled DNA was eluted in 50 µl of elution buffer (1 M sodium chloride, 50 mM Tris pH7.5). 16.6 µl of 45 SDS-PAGE sample buffer was added to the elution and 15 µl was separated on a 15% SDS-PAGE gel for Coomassie blue staining or immunoblot analysis.

Copper sensitivity assay

Mtb starter cultures were grown in 25 cm^2 flasks in Sauton's minimal media to an optical density between A_{580} 0.5 and 1.0. For each strain used, cultures were diluted to an A_{580} of 0.1 in Sauton's minimal media. 194 µl of diluted cultures were aliquoted into 96 well plates. 6 µl of $CuSO_4$ solution was added such that the final concentration of copper sulfate was 0, 100 or 500 µM. Each concentration for each strain was done in triplicate per experiment. OD_{580} readings were measured using a Molecular Devices plate spectrophotometer at day 0 and after 10 days of incubation at 37°C. Bacteria were inoculated onto 7H11 agar and incubated for 2–3 weeks for enumeration.

ICP-DRC-MS

10 ml cultures of WT, *pafA*, *mpa* or complemented strains were grown in 7H9 + ADN to an A_{580} of 2.0. 20 OD equivalents of bacteria were harvested by centrifugation and washed twice in 10 ml of 1 mM metal-free EDTA (EMD) to chelate all extracellular metal. Washed pellets were resuspended in 1 ml of 1 mM EDTA and transferred to centrifuge tubes. Cells were pelleted once more and resuspended in 100 µl of metal-free nitric acid (70%, Fisher). Cell suspensions were incubated overnight at 60°C and then cooled overnight. To neutralize the acid, 50 µl of metal free hydrogen peroxide was added. Finally, the volume was brought up to 3 ml with metal-free water. Total copper, zinc, and manganese analysis was performed via ICP-DRC-MS at Applied Speciation. Aliquots of each sample were introduced into a radio frequency plasma where energy-transfer processes cause desolvation, atomization and ionization. The ions are extracted from the plasma through a differentially-pumped vacuum interface and travel through a pressurized chamber (DRC) containing a specific reactive gas that preferentially reacts with interfering ions of the same target mass to charge ratios (m/z). A solid-state detector detects ions transmitted through the mass analyzer. Raw ICP-DRC-MS data was provided in µg/L. From this data, we determined the amount of metal in µg in the 3 mL preparations mentioned above. Because we used 20 OD bacteria equivalents, we were able to determine the µg/OD, and using the conversion of 1×10^7 colony forming units per 0.1 OD equivalent, we calculated the µg/CFU. Finally, we were able to convert the µg of metal into atoms using Avogadro's number and the molecular weight of the specific metal ion.

Supplementary Material

Refer to Web version on PubMed Central for supplementary material.

Acknowledgments

We thank Kristin Burns, David Giedroc, Ben Gold and Victor Torres for critical review of this manuscript. We thank Jiri Zavadil, Michael S. Glickman and Hideki Makinoshima for preliminary microarray studies and technical support. We thank Naoko Tanese for helpful suggestions. We are grateful to Ben Gold and Carl Nathan for the gift of antibodies to MymT. This work was supported by a Center For AIDS Research (CFAR) Pilot Project grant (NIH S P30 A1027742-17) and NIH grants AI065437 and HL92774 awarded to K.H.D., AI15447 to S.N.P., and AI 30036, 37856, and 36973 awarded to W.R.B. D.S. was supported by T32AI007180-27. We are grateful to C.N. for early support of this study (1R01HL72718). K.H.D was supported by a Burroughs Wellcome Investigator in the Pathogenesis of Infectious Disease award.

NIH-PA Author Manuscript

NIH-PA Author Manuscript

NIH-PA Author Manuscript

References

Bardarov S, Bardarov S Jr, Pavelka MS Jr, Sambandamurthy V, Larsen M, Tufariello J, Chan J, Hatfull G, Jacobs WR Jr. Specialized transduction: an efficient method for generating marked and unmarked targeted gene disruptions in *Mycobacterium tuberculosis*, M. bovis BCG and M. smegmatis. Microbiology 2002;148:3007–3017. [PubMed: 12368434]

Butler SM, Festa RA, Pearce MJ, Darwin KH. Self-compartmentalized bacterial proteases and pathogenesis. Mol Microbiol 2006;60:553–562. [PubMed: 16629660]

Camacho LR, Ensergueix D, Perez E, Gicquel B, Guilhot C. Identification of a virulence gene cluster of *Mycobacterium tuberculosis* by signature-tagged transposon mutagenesis. Mol Microbiol 1999;34:257–267. [PubMed: 10564470]

Cerda-Maira F, Darwin KH. The *Mycobacterium tuberculosis* proteasome: more than just a barrel-shaped protease. Microbes Infect 2009;11:1150–1155. [PubMed: 19671445]

Collins GA, Tansey WP. The proteasome: a utility tool for transcription? Curr Opin Genet Dev 2006;16:197–202. [PubMed: 16503126]

Cox JS, Chen B, McNeil M, Jacobs WR Jr. Complex lipid determines tissue-specific replication of *Mycobacterium tuberculosis* in mice. Nature 1999;402:79–83. [PubMed: 10573420]

Darwin KH. Prokaryotic ubiquitin-like protein (Pup), proteasomes and pathogenesis. Nat Rev Microbiol 2009;7:485–491. [PubMed: 19483713]

Darwin KH, Ehrt S, Gutierrez-Ramos JC, Weich N, Nathan CF. The proteasome of *Mycobacterium tuberculosis* is required for resistance to nitric oxide. Science 2003;302:1963–1966. [PubMed: 14671303]

Darwin KH, Lin G, Chen Z, Li H, Nathan CF. Characterization of a *Mycobacterium tuberculosis* proteasomal ATPase homologue. Mol Microbiol 2005;55:561–571. [PubMed: 15659170]

Farrow MF, Rubin EJ. Function of a mycobacterial major facilitator superfamily pump requires a membrane-associated lipoprotein. J Bacteriol 2008;190:1783–1791. [PubMed: 18156250]

Festa RA, Pearce MJ, Darwin KH. Characterization of the proteasome accessory factor (*paf*) operon in *Mycobacterium tuberculosis*. J Bacteriol 2007;189:3044–3050. [PubMed: 17277063]

Flynn JL, Chan J. Immunology of tuberculosis. Annu Rev Immunol 2001;19:93–129. [PubMed: 11244032]

Gandotra S, Schnappinger D, Monteleone M, Hillen W, Ehrt S. In vivo gene silencing identifies the *Mycobacterium tuberculosis* proteasome as essential for the bacteria to persist in mice. Nat Med 2007;13:1515–1520. [PubMed: 18059281]

Gold B, Deng H, Bryk R, Vargas D, Eliezer D, Roberts J, Jiang X, Nathan C. Identification of a copper-binding metallothionein in pathogenic mycobacteria. Nat Chem Biol 2008;4:609–616. [PubMed: 18724363]

Gold B, Rodriguez GM, Marras SA, Pentecost M, Smith I. The *Mycobacterium tuberculosis* IdeR is a dual functional regulator that controls transcription of genes involved in iron acquisition, iron storage and survival in macrophages. Mol Microbiol 2001;42:851–865. [PubMed: 11722747]

Gottesman S. Proteolysis in bacterial regulatory circuits. Annu Rev Cell Dev Biol 2003;19:565–587. [PubMed: 14570582]

Harlow, E.; Lane, DP. Antibodies: a laboratory manual. Cold Spring Harbor, NY: Cold Spring Harbor Laboratory Press; 1988.

Hatfull, GF.; Jacobs, WR. Molecular Genetics of Mycobacteria. ASM Press; 2000.

Hitomi Y, Outten CE, O'Halloran TV. Extreme zinc-binding thermodynamics of the metal sensor/regulator protein, ZntR. J Am Chem Soc 2001;123:8614–8615. [PubMed: 11525677]

Iwig JS, Chivers PT. DNA recognition and wrapping by *Escherichia coli* RcnR. J Mol Biol 2009;393:514–526. [PubMed: 19703465]

Kooperberg C, Sipione S, LeBlanc M, Strand AD, Cattaneo E, Olson JM. Evaluating test statistics to select interesting genes in microarray experiments. Hum Mol Genet 2002;11:2223–2232. [PubMed: 12217950]

Kosman DJ. Multicopper oxidases: a workshop on copper coordination chemistry, electron transfer, and metallophysiology. J Biol Inorg Chem 2010;15:15–28. [PubMed: 19816718]

NIH-PA Author Manuscript

NIH-PA Author Manuscript

NIH-PA Author Manuscript

Liu T, Ramesh A, Ma Z, Ward SK, Zhang L, George GN, Talaat AM, Sacchettini JC, Giedroc DP. CsoR is a novel *Mycobacterium tuberculosis* copper-sensing transcriptional regulator. Nat Chem Biol 2007;3:60–68. [PubMed: 17143269]

Ma Z, Cowart DM, Scott RA, Giedroc DP. Molecular insights into the metal selectivity of the copper(I)-sensing repressor CsoR from *Bacillus subtilis*. Biochemistry 2009a;48:3325–3334. [PubMed: 19249860]

Ma Z, Cowart DM, Ward BP, Arnold RJ, DiMarchi RD, Zhang L, George GN, Scott RA, Giedroc DP. Unnatural amino acid substitution as a probe of the allosteric coupling pathway in a mycobacterial Cu(I) sensor. J Am Chem Soc 2009b;131:18044–18045. [PubMed: 19928961]

Ma Z, Jacobsen FE, Giedroc DP. Coordination chemistry of bacterial metal transport and sensing. Chem Rev 2009c;109:4644–4681. [PubMed: 19788177]

Maciag A, Dainese E, Rodriguez GM, Milano A, Provvedi R, Pasca MR, Smith I, Palu G, Riccardi G, Manganelli R. Global analysis of the *Mycobacterium tuberculosis zur* (*furB*) regulon. J Bacteriol 2007;189:730–740. [PubMed: 17098899]

Mikolay A, Huggett S, Tikana L, Grass G, Braun J, Nies DH. Survival of bacteria on metallic copper surfaces in a hospital trial. Appl Microbiol Biotechnol. 2010

Outten CE, O'Halloran TV. Femtomolar sensitivity of metalloregulatory proteins controlling zinc homeostasis. Science 2001;292:2488–2492. [PubMed: 11397910]

Pearce MJ, Arora P, Festa RA, Butler-Wu SM, Gokhale RS, Darwin KH. Identification of substrates of the *Mycobacterium tuberculosis* proteasome. EMBO J 2006;25:5423–5432. [PubMed: 17082771]

Pearce MJ, Mintseris J, Ferreyra J, Gygi SP, Darwin KH. Ubiquitin-like protein involved in the proteasome pathway of *Mycobacterium tuberculosis*. Science 2008;322:1104–1107. [PubMed: 18832610]

Pieters J. *Mycobacterium tuberculosis* and the macrophage: maintaining a balance. Cell Host Microbe 2008;3:399–407. [PubMed: 18541216]

Rodriguez GM, Voskuil MI, Gold B, Schoolnik GK, Smith I. ideR, An essential gene in *Mycobacterium tuberculosis*: role of IdeR in iron-dependent gene expression, iron metabolism, and oxidative stress response. Infect Immun 2002;70:3371–3381. [PubMed: 12065475]

Sander P, Rezwan M, Walker B, Rampini SK, Kroppenstedt RM, Ehlers S, Keller C, Keeble JR, Hagemeier M, Colston MJ, Springer B, Bottger EC. Lipoprotein processing is required for virulence of *Mycobacterium tuberculosis*. Mol Microbiol 2004;52:1543–1552. [PubMed: 15186407]

Sato M, Bremner I. Oxygen free radicals and metallothionein. Free Radic Biol Med 1993;14:325–337. [PubMed: 8458590]

Saunders BM, Britton WJ. Life and death in the granuloma: immunopathology of tuberculosis. Immunol Cell Biol 2007;85:103–111. [PubMed: 17213830]

Serafini A, Boldrin F, Palu G, Manganelli R. Characterization of a *Mycobacterium tuberculosis* ESX-3 conditional mutant: essentiality and rescue by iron and zinc. J Bacteriol 2009;191:6340–6344. [PubMed: 19684129]

Siegrist MS, Unnikrishnan M, McConnell MJ, Borowsky M, Cheng TY, Siddiqi N, Fortune SM, Moody DB, Rubin EJ. Mycobacterial Esx-3 is required for mycobactin-mediated iron acquisition. Proc Natl Acad Sci U S A 2009;106:18792–18797. [PubMed: 19846780]

Smaldone GT, Helmann JD. CsoR regulates the copper efflux operon *copZA* in *Bacillus subtilis*. Microbiology 2007;153:4123–4128. [PubMed: 18048925]

Striebel F, Hunkeler M, Summer H, Weber-Ban E. The mycobacterial Mpa-proteasome unfolds and degrades pupylated substrates by engaging Pup's N-terminus. EMBO J 2010;29:1262–1271. [PubMed: 20203624]

Striebel F, Imkamp F, Sutter M, Steiner M, Mamedov A, Weber-Ban E. Bacterial ubiquitin-like modifier Pup is deamidated and conjugated to substrates by distinct but homologous enzymes. Nat Struct Mol Biol 2009;16:647–651. [PubMed: 19448618]

Tian J, Bryk R, Itoh M, Suematsu M, Nathan C. Variant tricarboxylic acid cycle in *Mycobacterium tuberculosis*: identification of alpha-ketoglutarate decarboxylase. Proc Natl Acad Sci U S A 2005;102:10670–10675. [PubMed: 16027371]

NIH-PA Author Manuscript

NIH-PA Author Manuscript

NIH-PA Author Manuscript

Wagner D, Maser J, Lai B, Cai Z, Barry CE 3rd, Honer Zu, Bentrup K, Russell DG, Bermudez LE. Elemental analysis of *Mycobacterium avium Mycobacterium tuberculosis*-, and *Mycobacterium smegmatis*-containing phagosomes indicates pathogen-induced microenvironments within the host cell's endosomal system. J Immunol 2005;174:1491–1500. [PubMed: 15661908]

Ward SK, Abomoelak B, Hoye EA, Steinberg H, Talaat AM. CtpV: a putative copper exporter required for full virulence of *Mycobacterium tuberculosis*. Mol Microbiol 77:1096–1110. [PubMed: 20624225]

Ward SK, Hoye EA, Talaat AM. The global responses of *Mycobacterium tuberculosis* to physiological levels of copper. J Bacteriol 2008;190:2939–2946. [PubMed: 18263720]

White C, Lee J, Kambe T, Fritsche K, Petris MJ. A role for the ATP7A copper-transporting ATPase in macrophage bactericidal activity. J Biol Chem 2009;284:33949–33956. [PubMed: 19808669]

NIH-PA Author Manuscript
NIH-PA Author Manuscript
NIH-PA Author Manuscript

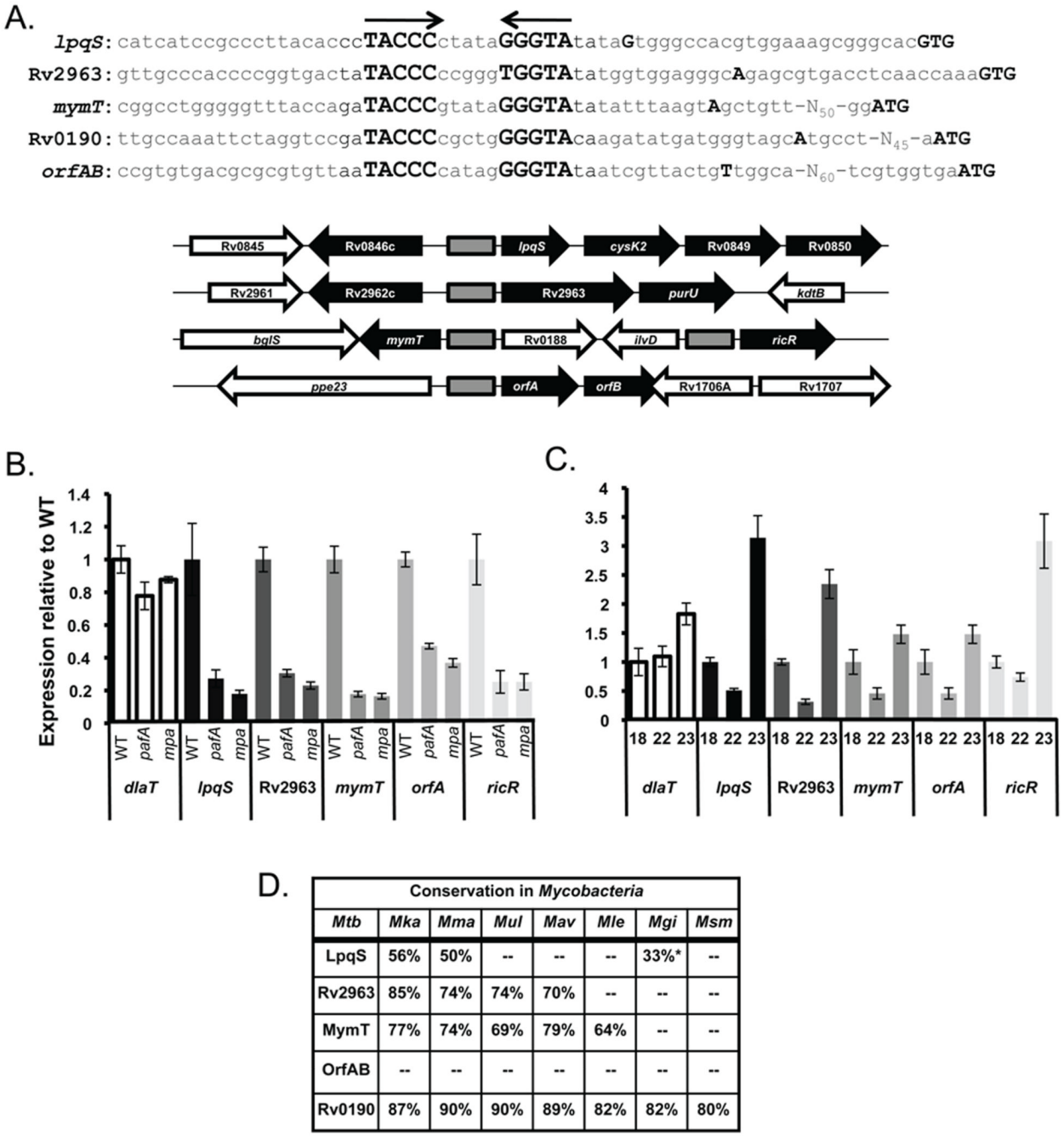

D.

Conservation in *Mycobacteria*							
Mtb	*Mka*	*Mma*	*Mul*	*Mav*	*Mle*	*Mgi*	*Msm*
LpqS	56%	50%	--	--	--	33%*	--
Rv2963	85%	74%	74%	70%	--	--	--
MymT	77%	74%	69%	79%	64%	--	--
OrfAB	--	--	--	--	--	--	--
Rv0190	87%	90%	90%	89%	82%	82%	80%

Fig. 1. Identification of a regulatory element in five loci repressed in proteasome degradation-defective *Mtb*

(A) Alignment of the *lpqS*, Rv2963, *mymT ricR*, and *orfAB* promoters. The putative transcriptional start sites as determined by 5'RACE are indicated by double-underlines, and the presumed start codons are at the 3' end of the sequence in capitals and in bold. The palindromic sequences are in bold and indicated by arrows. (Below) Genomic organization around each palindrome (gray boxes). Genes that were down-regulated in the *pafA* and *mpa* strains are in black arrows. (B) qRTPCR revealed that *ricR orfA* and *mymT* transcripts were decreased in *pafA* and *mpa* mutant strains when compared to WT *Mtb*. Transcript levels were normalized to *rpoB* (RNA polymerase β-subunit) for each gene in each condition or

NIH-PA Author Manuscript

NIH-PA Author Manuscript

NIH-PA Author Manuscript

strain tested. Fold changes relative to WT *Mtb* are plotted on the *y*-axis. Experiments are representative of three biological replicates, each performed in triplicate. *dlaT* (dihydrolipoamide acyltransferase, Rv2215) was used as a negative control. Transcript levels of *lpqS*, Rv2963, *mymT ricR*, and *orfAB* were significantly lower in the *pafA* and *mpa* mutants (Student's t-test, $p < 0.05$). (C) Complementation of the *mpa* mutation resulted in restoration of near WT levels of *lpqS*, Rv2963, *mymT ricR*, and *orfA* transcripts. Strains used for complementation were MHD18 (WT+pMV306, empty vector), MHD22 (*mpa* +pMV306), and MHD23 (*mpa*+pMV-*mpa*). The decreased levels in the *mpa* mutant were statistically significantly different from the WT and complemented strains. (D) Conservation of *lpqS*, Rv2963, *mymT, orfAB* and Rv0190 in other *Mycobacteria. Mka = M. kansasii, Mma = M. marinum*; *Mul = M. ulcerans*; *Mav = M. avium, Mle = M. leprae*, *Mka = M. kansansii, Mgi = M. gilvum*, *Msm = M. smegmatis*. The asterisk (*) signifies the homologue did not have the palindromic sequence found upstream of *Mtb lpqS*.

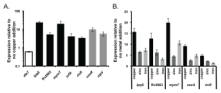

Fig. 2. Genes repressed in *pafA* and *mpa* mutants are copper inducible

(A) Induction of genes in response to 500 μM $CuSO_4$ for four hours. The genes repressed in the proteasome degradation-defective strains (in black) were all significantly induced in WT *Mtb* (H37Rv) in response to copper as shown by qRTPCR. *csoR* and *ctpV* are known copper-inducible genes that were used as positive controls. *dlaT* served as a negative control. (B) In WT *Mtb*, *lpqS*, Rv2963, *mymT*, *ricR*, and *orfA* were significantly induced by 500 μM $CuSO_4$, 10-fold more iron (0.05% w/v ferric ammonium citrate) and 500 μM $ZnSO_4$ when compared to untreated samples grown in Sauton's minimal media. *ricR* transcripts appear to have the lowest response to the metals tested. Data are representative of two biological replicates, each performed in triplicate.

NIH-PA Author Manuscript NIH-PA Author Manuscript NIH-PA Author Manuscript

NIH-PA Author Manuscript
NIH-PA Author Manuscript
NIH-PA Author Manuscript

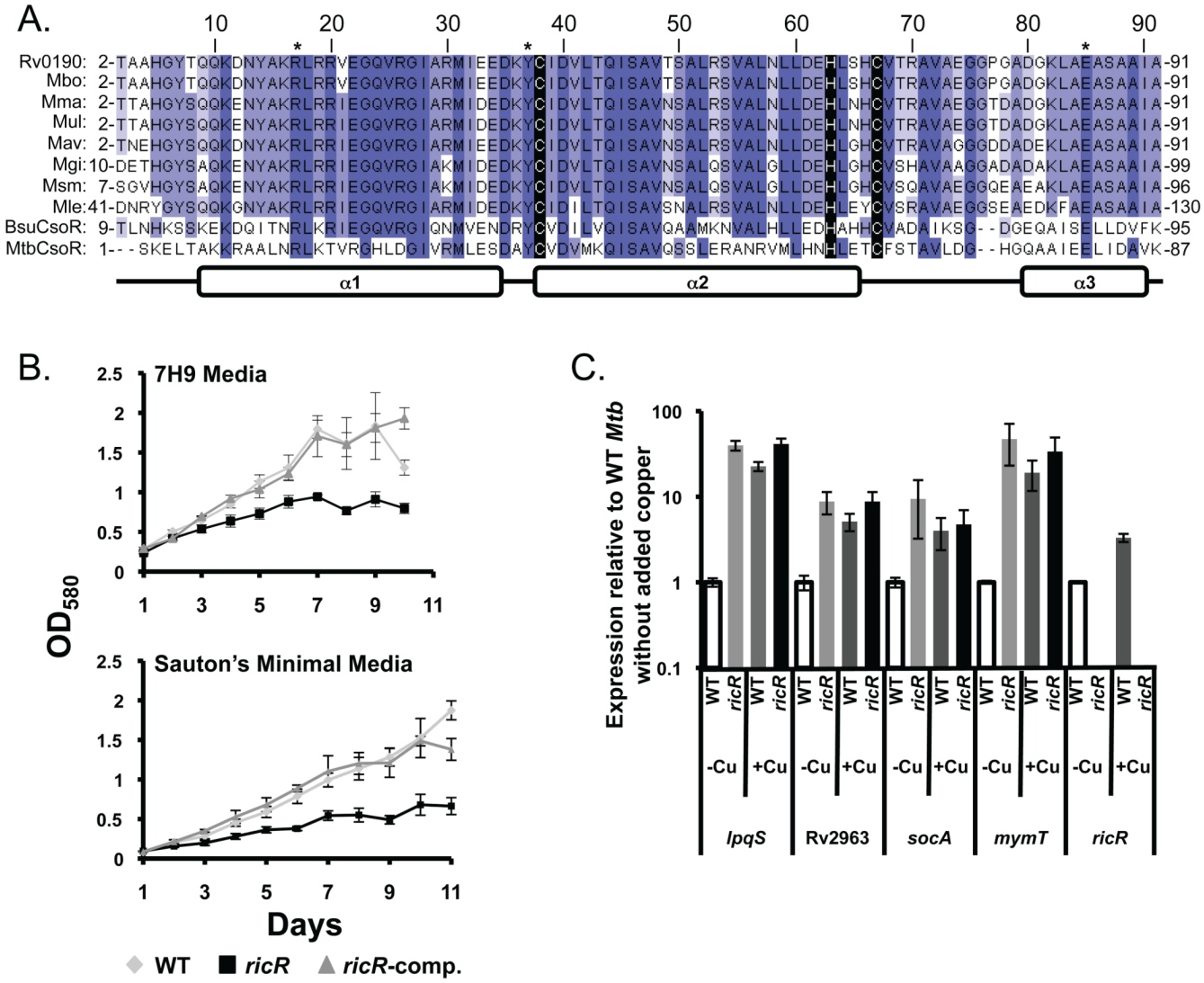

Fig. 3. RicR is a copper-responsive regulator

(A) Alignment of RicR (Rv0190/MT0200) homologues in other *Mycobacteria* along with *Mtb*CsoR, and *Bsu*CsoR. Gene identification: *Mbo*, Mb0196; *Mma*, MMAR_0433; *Mul*, MUL_1083; *Mav*, MAV_4988; *Mgi*, Mflv_0484; *Msm*, MSMEG_0230; *Mle*, ML2609. In black is conserved copper coordinating amino acids [cysteine (Cys) 38, histidine 63, Cys67] based on the crystal structure of *Mtb*CsoR (Liu et al., 2007). The asterisk (*) indicates amino acids predicted to be important for DNA interactions in *Mtb*CsoR (Ma et al., 2009a, Liu et al., 2007). Secondary structure prediction (alpha helices 1–3) was adapted from (Liu et al., 2007). Increasing blue intensity indicates increasing conservation of the highlighted amino acids. (B) Growth curves comparing the WT, *ricR* transposon mutant, and *ricR*-complemented strains in 7H9+ADN media (6 μM $CuSO_4$) and Sauton's minimal media (trace copper). OD_{580} was measured daily. These experiments represent three independent experiments, each done in duplicate. (C) *lpqS*, Rv2963, *orfA*, and *mymT* are highly expressed in the *ricR* mutant, comparable to levels in copper-induced WT bacteria. Cultures were grown in Sauton's minimal media until to OD_{580} of ~0.6, after which RNA was harvested for analysis. For copper treatment, cells were treated for four hours with 500 μM $CuSO_4$ prior to RNA harvest. *ricR* transcript was not detected (ND) in the *ricR* mutant due

NIH-PA Author Manuscript

NIH-PA Author Manuscript

NIH-PA Author Manuscript

to disruption by the transposon insertion. qRTPCR was performed as described in the *Experimental Procedures* and Fig. 1. This is representative of two experiments, each done in triplicate.

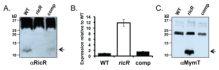

Fig. 4. Complementation of the *ricR* mutation

(A) Immunoblot analysis shows that RicR levels were partially restored in the *ricR*-complemented strain grown in Sauton's minimal media. Non-specific bands recognized by the RicR polyclonal antibodies served as loading controls. Data are representative of three biological replicates. (B) *lpqS* transcript levels at early stationary phase were highly expressed in the *ricR* mutant compared to WT *Mtb* and were restored to WT levels in the *ricR*-complemented strain. Bacteria were grown in Sauton's minimal media for these experiments and this is representative of two biological replicates performed in triplicate. (C) Immunoblot analysis showed MymT levels were markedly increased in the *ricR* mutant and were restored to undetectable levels in the complemented strain grown in Sauton's minimal media. Cross-reactive proteins served as the loading control.

NIH-PA Author Manuscript NIH-PA Author Manuscript NIH-PA Author Manuscript

NIH-PA Author Manuscript

NIH-PA Author Manuscript

NIH-PA Author Manuscript

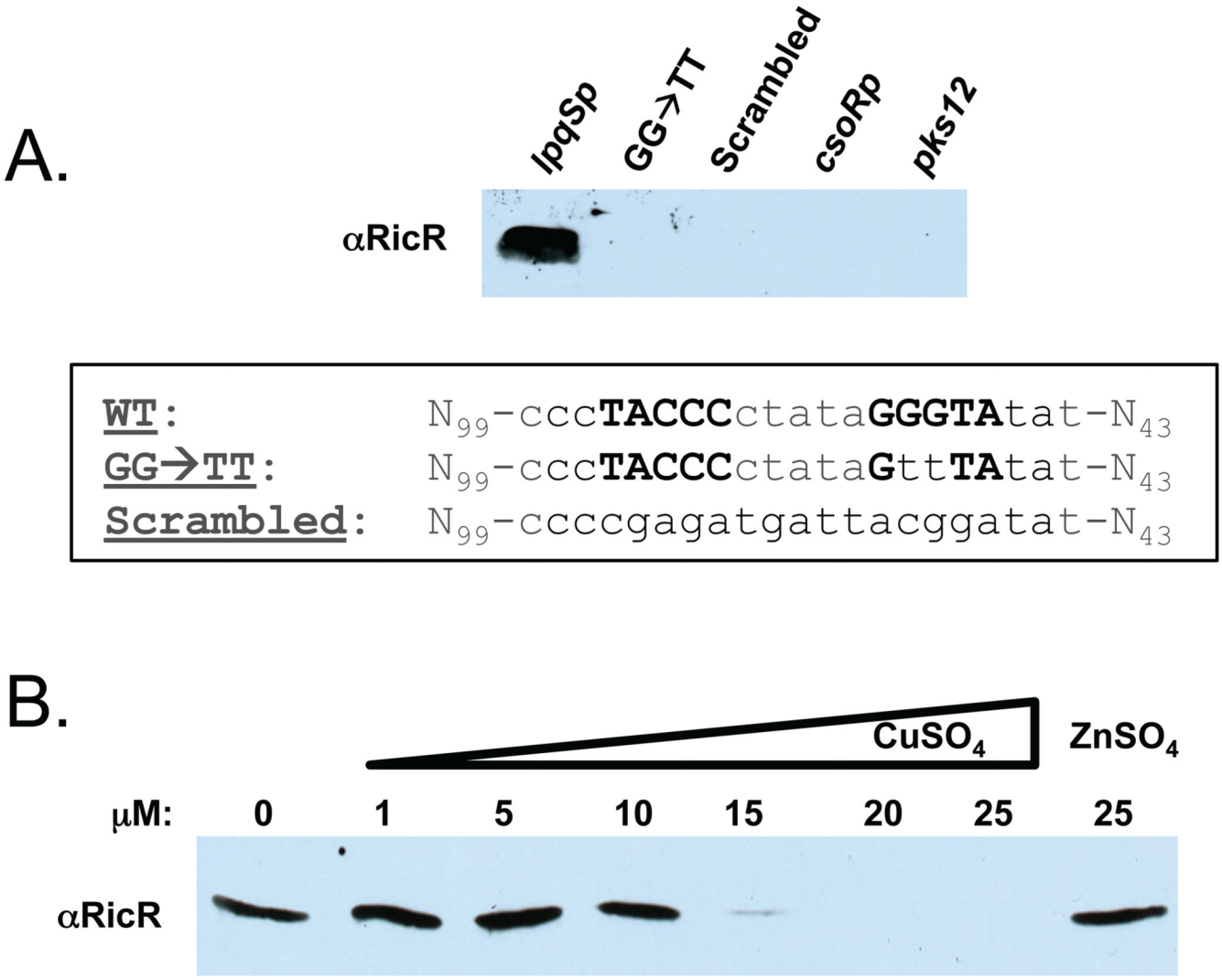

Fig. 5. RicR binds the *lpqS* promoter

(A) DNA affinity chromatography revealed RicR associates with the *lpqS* promoter (*lpqSp*). Clarified lysates of *E. coli* expressing untagged *ricR* were incubated with biotinylated DNA (see Experimental Procedures for details). RicR-DNA interaction was disrupted upon palindrome mutagenesis (sequences indicated below). RicR did not bind the *csoR* promoter (*csoRp*) or intragenic DNA (*pks12*). (B) Copper disrupted the RicR-DNA interaction in a dose-dependent manner.

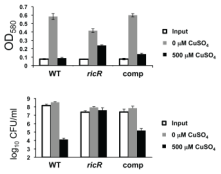

Fig. 6. The *ricR* mutant is hyper-resistant to copper toxicity

Copper sensitivity assay comparing the ability of WT, *ricR* and *ricR*-complemented *Mtb* strains to survive in 500 μM copper sulfate. The bottom panel shows colony-forming units (CFU) per ml from the same experiment. Data are representative of at least two experiments, each done in triplicate. CFU after 10 days in untreated versus copper-treated *ricR* strain were not statistically significantly different (Student's t-test, $p > 0.05$), while the WT and complemented strains had significantly fewer CFU between copper-treated and untreated cultures.

NIH-PA Author Manuscript
NIH-PA Author Manuscript
NIH-PA Author Manuscript

NIH-PA Author Manuscript

NIH-PA Author Manuscript

NIH-PA Author Manuscript

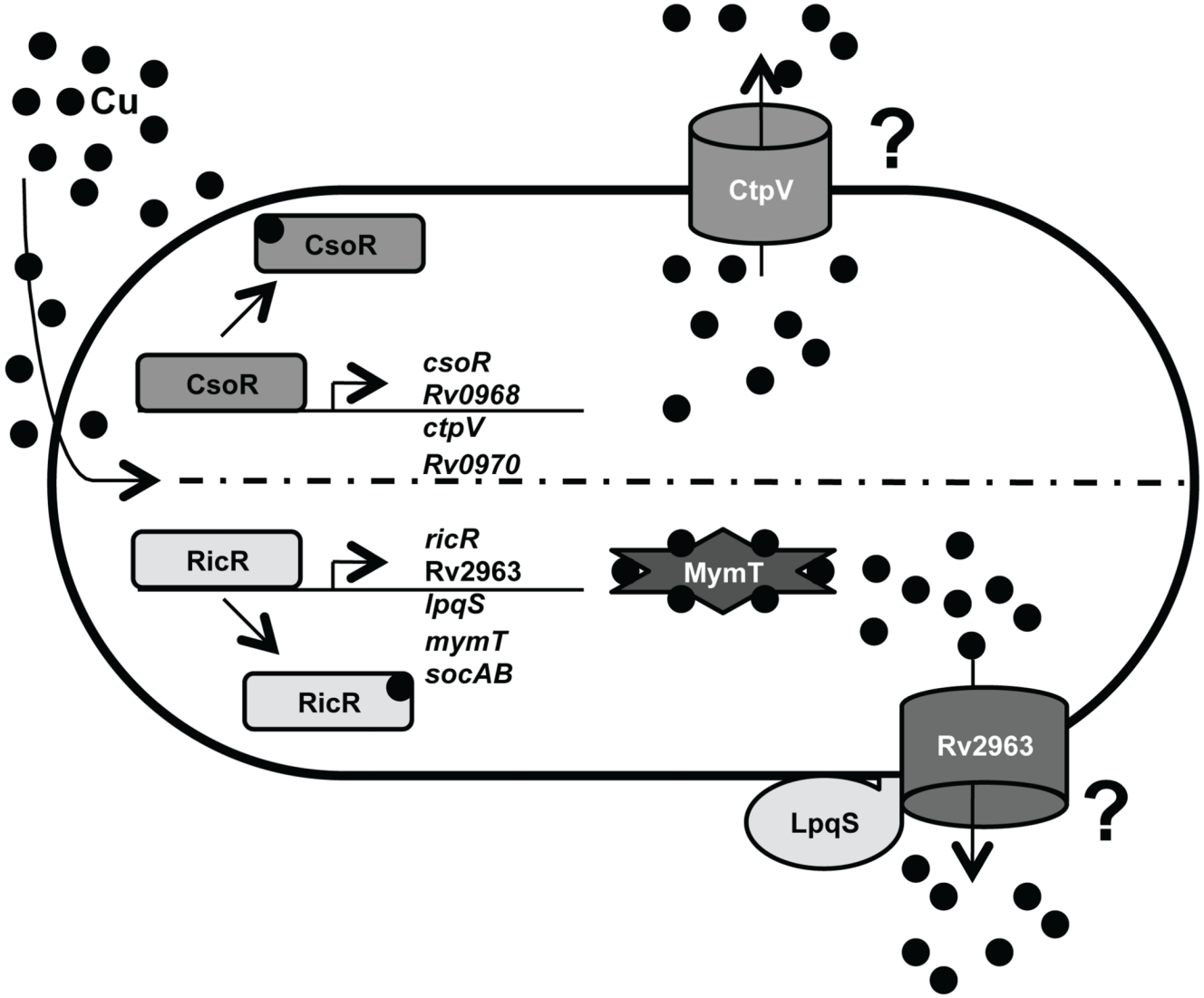

Fig. 7. Model for a dual copper response in *Mtb*

Two parallel pathways appear to respond to copper in *Mtb*. (Top half) Copper induces the release of CsoR from its own promoter, resulting in the expression of *ctpV*, a predicted P-type ATPase metal transporter. (Bottom half) Copper also de-represses RicR from its own promoter as well as four other promoters. MymT binds up to six Cu(I) ions and may play a role in the sequestration or transport of excess copper. Rv2963 and LpqS are predicted to be membrane associated proteins and may play a role in copper export.

NIH-PA Author Manuscript NIH-PA Author Manuscript NIH-PA Author Manuscript

Mol Microbiol. Author manuscript; available in PMC 2012 January 1.

Table 1

Genes more than two-fold up-regulated in *pafA*, *mpa*, and *mpa607* mutants as determined by microarray analysis[a], sorted by locus.

Locus	Gene Name[b]	*mpa607*[c]	*mpa*[c]	*pafA*[c]	Zur Regulon[d]	IdeR regulated[e]
Rv0106	hypothetical protein	2.27	3.25	4.21	+	
Rv0280	PPE FAMILY PROTEIN (*ppe3*)	3.74	3.85	4.10	+	+
Rv0281	hypothetical protein	1.97	1.94	2.46	+	+
Rv0282	hypothetical protein	2.42	2.15	2.49	+	+
Rv0282	hypothetical protein	1.94	2.00	2.62	+	+
Rv0283	POSSIBLE CONSERVED MEMBRANE PROTEIN	1.80	2.06	2.34	+	+
Rv0284	POSSIBLE CONSERVED MEMBRANE PROTEIN	2.25	2.33	2.51	+	+
Rv0285	PE FAMILY PROTEIN (*pe5*)	1.82	1.91	2.19	+	+
Rv0286	PPE FAMILY PROTEIN (*ppe4*)	1.56	1.85	2.16	+	+
Rv0287	ESAT-6 LIKE PROTEIN (*esxG*)	1.73	1.61	2.10	+	+
Rv0289	hypothetical protein	1.93	2.00	2.20	+	+
Rv0290	PROBABLE CONSERVED TRANSMEMBRANE PROTEIN	1.68	1.94	1.96	+	+
Rv0292	PROBABLE CONSERVED TRANSMEMBRANE PROTEIN	1.70	1.89	2.13	+	+
Rv0885	hypothetical protein	1.92	1.75	2.49		
Rv2055c	Probable ribosomal protein S18 (*rpsR2*)	2.63	2.65	3.81	+	
Rv2056c	Probable ribosomal protein S14 (*rpsN2*)	2.68	2.43	4.21	+	
Rv2057c	Probable ribosomal protein L33 (*rpmG1*)	2.94	2.91	4.20	+	
Rv2058c	Probable 50S ribosomal protein L28 (*rpmB2*)	4.15	3.47	6.12	+	
Rv2059	hypothetical protein	1.66	NaN	2.17	+	
Rv2359	*zur*	0.69	0.54	0.94		
Rv3074	hypothetical protein	2.57	1.76	1.87		

[a] Dye-flipped experiments were performed in duplicate for each mutant compared to WT. Statistical analysis was determined by SAM analysis between all conditions.

[b] Functional annotations are taken from the *Mtb* strain H37Rv complete genome sequence (www.jcvi.org)

[c] Numbers represent expression in the mutant strains relative to WT *Mtb* in 7H9 media grown to early stationary phase

[d] (Maciag et al., 2007)

NIH-PA Author Manuscript

NIH-PA Author Manuscript

NIH-PA Author Manuscript

[e](Rodriguez et al., 2002)

NIH-PA Author Manuscript
NIH-PA Author Manuscript
NIH-PA Author Manuscript

Table 2

Genes more than two-fold down-regulated in *pafA*, *mpa*, and *mpa607* mutants as determined by microarray analysisa, sorted by locus.

Locus	Gene Name[b]	*mpa607*[c]	*mpa*[c]	*pafA*[c]
Rv0140	hypothetical protein	0.40	0.56	0.48
Rv0654	PROBABLE DIOXYGENASE	0.34	0.41	0.49
Rv0765c	PROBABLE OXIDOREDUCTASE	0.48	0.65	0.54
Rv0766c	PROBABLE CYTOCHROME P450 123 (*cyp123*)	0.41	0.47	0.54
Rv0767c	hypothetical protein	0.28	0.49	0.47
Rv0768	PROBABLE ALDEHYDE DEHYDROGENASE NAD DEPENDENT ALDA (*aldA*)	0.38	0.48	0.46
Rv0769	PROBABLE DEHYDROGENASE/REDUCTASE	0.47	0.53	0.51
Rv0790c	hypothetical protein	0.45	0.58	0.50
Rv0791c	hypothetical protein	0.39	0.52	0.39
Rv0792c	PROBABLE TRANSCRIPTIONAL REGULATORY PROTEIN (PROBABLY GNTR-FAMILY)	0.37	0.55	0.50
Rv0793	hypothetical protein	0.47	0.67	0.56
Rv0847	**PROBABLE LIPOPROTEIN (*lpqS*)**	**0.24**	**0.52**	**0.33**
Rv0848	POSSIBLE CYSTEINE SYNTHASE A (*cysK2*)	0.32	0.56	0.42
Rv0850	PUTATIVE TRANSPOSASE (FRAGMENT)	0.33	0.70	0.39
Rv1169c	PE FAMILY PROTEIN (*pe11*)	0.41	0.66	0.54
Rv1218c	PROBABLE TETRONASIN-TRANSPORT ATP-BINDING PROTEIN ABC TRANSPORTER	0.32	0.67	0.40
Rv1285	PROBABLE SULFATE ADENYLYLTRANSFERASE SUBUNIT 2 (*cysD*)	0.24	0.41	0.35
Rv1286	PROBABLE BIFUNCTIONAL ENZYME CYSN/CYSC (*cysN*)	0.30	0.54	0.37
Rv1287	hypothetical protein	0.44	0.67	0.44
Rv2466c	hypothetical protein	0.34	0.49	0.45
Rv2517c	hypothetical protein	0.43	0.52	0.54
Rv2641	CADMIUM INDUCIBLE PROTEIN (*cadI*)	0.47	0.63	0.50
Rv2642	POSSIBLE TRANSCRIPTIONAL REGULATORY PROTEIN (PROBABLY ARSR-FAMILY)	0.39	0.53	0.46
Rv2873	CELL SURFACE LIPOPROTEIN (*mpt83*)	0.46	0.52	0.54
Rv2875	MAJOR SECRETED IMMUNOGENIC PROTEIN (*mpt70*)	0.40	0.42	0.41
Rv2912c	PROBABLE TRANSCRIPTIONAL REGULATORY PROTEIN (PROBABLY TETR-FAMILY)	0.26	0.42	0.25
Rv2913c	POSSIBLE D-AMINO ACID AMINOHYDROLASE (D-AMINO ACID HYDROLASE)	0.23	0.41	0.36
Rv2962c	POSSIBLE GLYCOSYL TRANSFERASE	0.41	0.64	0.51
Rv2963	**PROBABLE INTEGRAL MEMBRANE PROTEIN**	**0.25**	**0.60**	**0.38**
Rv2987c	PROBABLE 3-ISOPROPYLMALATE DEHYDRATASE (SMALL SUBUNIT) (*leuD*)	0.56	0.40	0.43
Rv3249c	POSSIBLE TRANSCRIPTIONAL REGULATORY PROTEIN (PROBABLY TETR-FAMILY)	0.34	0.46	0.42
Rv3250c	PROBABLE RUBREDOXIN (*rubB*)	0.37	0.50	0.46
Rv3251c	PROBABLE RUBREDOXIN (*rubA*)	0.34	0.50	0.47
Rv3252c	PROBABLE TRANSMEMBRANE ALKANE 1-MONOOXYGENASE (*alkB*)	0.30	0.45	0.43
Rv3269	hypothetical protein	0.40	0.65	0.59
Rv3270	PROBABLE METAL CATION-TRANSPORTING P-TYPE ATPASE C (*ctpC*)	0.37	0.63	0.51
Rv3463	hypothetical protein	0.37	0.53	0.48
MT0196	***mymT***	**0.36**	**0.71**	**0.47**

[a] Dye-flipped experiments were performed in duplicate for each mutant compared to WT. Statistical analysis was determined by SAM analysis between all conditions.

[b] Functional annotations are taken from the *Mtb* strain H37Rv complete genome sequence (www.jcvi.org)

[c] Numbers represent expression in the mutant strains relative to WT *Mtb* in 7H9 media grown to early stationary phase

[d] In bold are genes with the palindrome.

NIH-PA Author Manuscript
NIH-PA Author Manuscript
NIH-PA Author Manuscript

NIH-PA Author Manuscript

NIH-PA Author Manuscript

NIH-PA Author Manuscript

Table 3

Genes differentially regulated in a Δ*csoR::hyg* mutant.

locus	*gene*	Name[c]	Cu−[a]	Cu+[b]
Rv0967	*csoR*	hypothetical protein	0.09	0.02
Rv0968		hypothetical protein	6.41	0.12
Rv0969	*ctpV*	PROBABLE METAL CATION TRANSPORTER P-TYPE ATPASE CTPV	4.55	0.14
Rv0970		PROBABLE CONSERVED INTEGRAL MEMBRANE PROTEIN	1.66	0.21

[a] Numbers represent average fold-change in the Δ*csoR::hyg* mutant compared to WT in the absence of copper. These data represents 2 dye-flip experiments after SAM analysis.

[b] Numbers represent average fold-change in the Δ*csoR::hyg* mutant compared to WT in the presence of copper. These data represents 2 dye-flip experiments after SAM analysis.

[c] Functional annotations are taken from the *M. tuberculosis* H37Rv complete genome sequence (www.jcvi.org)

NIH-PA Author Manuscript NIH-PA Author Manuscript NIH-PA Author Manuscript

Table 4

Genes differentially regulated in a *ricR* mutant compared to WT *Mtb* with and without copper[a].

CDC1551	H37Rv	*gene*	Name	Cu−[a]	Cu+[b]
MT0195	Rv0186	*bglS*	beta-glucosidase, putative	15.94	3.29
MT0196	**NA**	***mymT***	**hypothetical protein**	**106.18**	**2.04**
MT0200	**Rv0190**	***ricR***	**homologue of copper sensitive operon repressor *csoR***	**4.74**	**−1.50**
MT1746.1	**NA**	***socB***	**hypothetical protein**	**16.22**	**2.62**
MT0868	NA		hypothetical protein	6.59	1.26
MT0869	Rv0846c		copper-binding protein, putative	13.53	1.83
MT0870	**Rv0847**	***lpqS***	**hypothetical protein**	**44.45**	**2.27**
MT0871	Rv0848	*cysK2*	cysteine synthase/cystathionine beta-synthase family protein	33.63	2.04
MT0872	Rv0849		Probable conserved integral membrane transport protein	27.26	2.35
MT0873	Rv0850		IS1606', transposase	10.58	2.28
MT3038	Rv2962c	*Rv2962c*	UDP-glucoronosyl andUDP-glucosyltransferase family proteins	13.34	1.95
MT3039	**Rv2963**		**hypothetical protein**	**41.00**	**3.77**
MT3041	Rv2964	*purU*	formyltetrahydrofolate deformylase	15.23	5.95
MT3041.1	NA		hypothetical protein	5.31	2.63
MT3159	Rv3074		hypothetical protein	5.42	5.21
MT3885	Rv3776		hypothetical protein	8.21	8.50
MT1422	Rv1378c		hypothetical protein	11.34	7.12
MT1511	Rv1464		aminotransferase, class V	4.30	3.13
MT3753.2	NA		hypothetical protein	3.40	6.47

[a] Numbers represent average fold-change over 2 dye-flip experiments after SAM analysis.

[b] Numbers represent average fold-change over 3 dye-flip experiments after SAM analysis.

[c] Functional annotations are taken from the *Mtb* strain H37Rv complete genome sequence (www.jcvi.org)

[d] Genes with the palindromic sequence in their promoters are in bold.

Mol Microbiol. Author manuscript; available in PMC 2012 January 1.